JVI Journals.ASM.org

Arterivirus Minor Envelope Proteins Are a Major Determinant of Viral Tropism in Cell Culture

Debin Tian,[a] Zuzhang Wei,[a] Jessika C. Zevenhoven-Dobbe,[b] Runxia Liu,[a] Guangzhi Tong,[a] Eric J. Snijder,[b] and Shishan Yuan[a]

Department of Swine Infectious Diseases, Shanghai Veterinary Research Institute, Chinese Academy of Agricultural Sciences, Shanghai, China,[a] and Molecular Virology Laboratory, Department of Medical Microbiology, Center of Infectious Diseases, Leiden University Medical Center, Leiden, The Netherlands[b]

Arteriviruses are enveloped positive-strand RNA viruses for which the attachment proteins and cellular receptors have remained largely controversial. Arterivirus particles contain at least eight envelope proteins, an unusually large number among RNA viruses. These appear to segregate into three groups: major structural components (major glycoprotein GP5 and membrane protein [M]), minor glycoproteins (GP2a, GP3, and GP4), and small hydrophobic proteins (E and the recently discovered ORF5a protein). Biochemical studies previously suggested that the GP5-M heterodimer of porcine reproductive and respiratory syndrome virus (PRRSV) interacts with porcine sialoadhesin (pSn) in porcine alveolar macrophages (PAM). However, another study proposed that minor protein GP4, along with GP2a, interacts with CD163, another reported cellular receptor for PRRSV. In this study, we provide genetic evidence that the minor envelope proteins are the major determinant of arterivirus entry into cultured cells. A PRRSV infectious cDNA clone was equipped with open reading frames (ORFs) encoding minor envelope and E proteins of equine arteritis virus (EAV), the only known arterivirus displaying a broad tropism in cultured cells. Although PRRSV and EAV are only distantly related and utilize diversified transcription-regulating sequences (TRSs), a viable chimeric progeny virus was rescued. Strikingly, this chimeric virus (vAPRRS-EAV2ab34) acquired the broad *in vitro* cell tropism of EAV, demonstrating that the minor envelope proteins play a critical role as viral attachment proteins. We believe that chimeric arteriviruses of this kind will be a powerful tool for further dissection of the arterivirus replicative cycle, including virus entry, subgenomic RNA synthesis, and virion assembly.

The *Arteriviridae*, which are enveloped RNA viruses with a polycistronic positive-stranded genome, together with the *Coronaviridae* and *Roniviridae*, belong to the order *Nidovirales* (2). The arterivirus family consists of equine arteritis virus (EAV), porcine reproductive and respiratory syndrome virus (PRRSV), lactate dehydrogenase-elevating virus (LDV), and simian hemorrhagic fever virus (SHFV) (42). PRRSV isolates segregate into European (type I) and North American (type II) genotypes, which share only about 60% sequence identity (32). In general, the host range of arteriviruses is very restricted: EAV is only known to infect horses and donkeys; the tropism of PRRSV is specific for swine; LDV infects only mice; and SHFV targets several genera of monkeys, in which it can cause either acute or persistent infections (42). PRRSV infection, in particular, often leads to high-mortality disease outbreaks and is considered one of the greatest threats to the swine industry worldwide (24, 33, 48, 64). Recently, a large outbreak of highly virulent PPRSV (type II) affected the Asian swine industry, causing considerable economic losses (48, 64).

The arterivirus genome is a polyadenylated RNA molecule of about 12 to 16 kb (see Fig. 1), comprising short 5′- and 3′-terminal untranslated regions (UTRs) flanking a large replicase gene (open reading frame 1a [ORF1a] and ORF1b) and—in the case of PRRSV, EAV, and LDV—eight known structural protein genes (17, 19, 42, 43). The SHFV genome contains four additional ORFs, which appear to be derived from an ancient duplication of ORFs 2a to 4 and may encode additional envelope proteins (18). Like coronaviruses, arteriviruses employ a unique mechanism of discontinuous RNA synthesis to produce an extensive nested set of subgenomic (sg) mRNAs. These transcripts are 3′ coterminal but also carry a common 5′ leader sequence that is identical to the 5′-terminal part of the genome (37). Synthesis of sg mRNA is thought to start with the generation of subgenome-length negative-stranded templates, one for each mRNA species, which derive from a process of discontinuous negative-strand synthesis directed by short, conserved transcription-regulating sequences (TRSs). During discontinuous RNA synthesis, the genomic 3′-proximal region is copied up to a so-called body TRS (TRS-B), after which RNA synthesis is interrupted and the 3′ end of the nascent negative strand base pairs to a complementary sequence (leader TRS [TRS-L]) in the 5′ UTR. Following the base-pairing interaction between the negative-stranded TRS-B and the positive-stranded TRS-L, RNA synthesis is resumed to add the complement of the leader sequence to the subgenome-length negative-stranded RNA, which can subsequently serve as a template for mRNA synthesis (7, 26, 37–39, 46).

EAV and PRRSV are the most extensively studied arteriviruses. Replicase ORF1a and ORF1ab, via ribosomal frameshift-mediated translational reprogramming, encode the nonstructural polyproteins pp1a and pp1ab, which ultimately mature into the 13 or 14 nonstructural proteins (nsp's) that direct genome replication and sg mRNA synthesis (16, 65). The structural-protein-coding region generates glycoprotein GP2a or GP2b (encoded by ORF2a in PRRSV type II and by ORF2b in EAV and PRRSV type I), the envelope protein E (encoded by ORF2b in PRRSV type II and by ORF2a in EAV and PRRSV type I), GP3 (ORF3), GP4 (ORF4),

Received 17 November 2011 **Accepted** 6 January 2012
Published ahead of print 18 January 2012
Address correspondence to Shishan Yuan, shishanyuan@hotmail.com, or Eric J. Snijder, e.j.snijder@lumc.nl.

doi:10.1128/JVI.06836-11

GP5 (ORF5), membrane protein M (ORF6), and nucleocapsid protein N (ORF7) (42, 44). Recently, an additional small hydrophobic protein, which is encoded by an ORF (ORF5a) overlapping the GP5-coding sequence, was identified (17, 19). This ORF5a protein was identified in PRRSV particles, and its expression was found to be important for the efficient production of EAV progeny virus, although an ORF5a knockout mutant retained a moderate level of infectiousness (17, 19). Previously, the expression of all other genes in the 3′ quarter of the EAV genome (ORFs 2a to 7) was found to be essential for the production of infectious virus particles, although knockouts of ORFs 2a to 4 were found to produce virus-like particles containing the three major structural proteins (GP5, M, and N) and RNA (28, 59, 63). Consequently, the minor envelope proteins (GP2a and -b, GP3, GP4, and E), which may form different oligomeric complexes, were postulated to be critical determinants of arterivirus infection, e.g., by controlling virus attachment or entry (15, 41, 58, 60). However, thus far, little is known about the structural properties of arterivirus proteins and their functional interactions with each other and with host factors.

Arterivirus entry relies on receptor-mediated endocytosis, but the identities of the cellular receptor(s) and the viral attachment protein(s) have remained controversial (3, 22, 30, 49). Although PRRSV and EAV infect cells from the monocyte/macrophage lineage in their natural hosts, they display different tropisms in cell culture (14, 42). EAV can productively infect a wide variety of cell lines, including baby hamster kidney (BHK-21), African green monkey kidney (Vero and MA-104), rabbit kidney (RK-13), and even human kidney (43) cells. On the other hand, PRRSV can infect only MA-104 cells and cells of its derivative line, MARC-145 (20, 42). The most extensively documented PRRSV receptor is porcine sialoadhesin (pSn) in porcine alveolar macrophages (PAM) (5, 6, 12, 13, 51). Expression of pSn can render the nonpermissive PK-15 cell line susceptible to PRRSV entry, but the internalized virus is not uncoated (51). The conclusion that pSn is the (primary) PRRSV receptor was challenged on the grounds that the protein is not expressed by MARC-145 cells, which are permissive to PRRSV infection (13). Through screening of a PAM cDNA library, the membrane protein CD163 was identified as an additional determinant of PRRSV entry (1). The CD163 molecule can confer susceptibility to PRRSV infection on nonpermissive cells and is expressed in MARC-145 cells. Strikingly, different potential PRRSV attachment proteins have been proposed in conjunction with the different potential receptors. The GP5-M complex was identified as the likely attachment protein in view of its capacity to bind pSn in a sialic acid-dependent manner *in vitro* (50). However, another study documented that the minor envelope proteins GP2 and GP4 interact with CD163 *in vitro* (4). Van Breedam and coworkers proposed a model in which pSn and CD163 would together mediate PRRSV entry, with the former serving as the authentic receptor for adsorption and the latter subsequently mediating penetration (49). Nevertheless, it is clear that more genetic and biochemical information is required to clarify the exact roles of the different viral and cellular proteins claimed to be involved. Such information will also be key for the rational design of vaccines and antivirals.

In this study, we provide genetic evidence that the minor envelope proteins GP2, GP3, GP4, and E together play a key role in the entry of arteriviruses into cultured cells. Utilizing PRRSV and EAV infectious cDNA clones (52, 62), we constructed a chimera in which PRRSV ORFs 2a to 4 were replaced by the corresponding genes from EAV. Viable chimeric virus was rescued following transfection of this cDNA clone. Moreover, this chimeric PRRSV acquired the broad cell tropism that is typical of its minor envelope protein donor, EAV. For example, besides MARC-145, the chimeric virus could productively infect both the BHK-21 and Vero cell lines, which are not permissive for infection with wild-type PRRSV. This strongly suggests that the tropism and entry of PRRSV, and likely also of other arteriviruses, are mediated by the minor rather than the major envelope proteins. This finding enhances our understanding of arterivirus entry and may be of great significance for the rational design of PRRSV vaccines and antiviral compounds.

MATERIALS AND METHODS

Cells, viruses, and antibodies. The MARC-145 and Vero cell lines (ATCC, Manassas, VA) were cultured in Eagle's minimal essential medium (EMEM) with 10% fetal bovine serum (FBS; Gibco-BRL, MD) and were maintained in EMEM with 2% FBS. The BHK-21 cell line (ATCC) was cultured in modified Eagle medium (MEM) with 10% FBS (Gibco-BRL) and was maintained in MEM with 2% FBS. PAM were obtained from a 4-week-old PRRSV-negative piglet as described previously (57) and were cultured in RPMI 1640 (Gibco-BRL) with 10% FBS. All the cells were cultured in an incubator at 37°C under 5% CO_2. The wild-type PRRSV strain vAPRRS was derived from infectious cDNA clone pAPRRS (GenBank accession no. GQ330474). The wild-type EAV strain vEAV030 was derived from infectious cDNA clone pEAV030 (NC002532). Monoclonal antibodies (MAbs) specific for the PRRSV N protein (N-MAb) and nonstructural protein 2 (nsp2-MAb) were kindly provided by Ying Fang (South Dakota State University). A rabbit antiserum recognizing EAV nsp2 has been described previously (45), and an anti-EAV GP2b serum (ARV-EAV-GP2b, recognizing the MSPSRRTSSGTLPRRKIL peptide) was obtained from Shanghai GL Biochem (Shanghai, China). The secondary antibodies, Alexa Fluor 568-labeled goat anti-mouse IgG and Alexa Fluor 555-labeled goat anti-rabbit IgG, were purchased from Molecular Probes (Invitrogen, CA).

Construction of chimeric full-length cDNA clones. To obtain a convenient DNA-based system in which to launch recombinant EAV and PRRSV, the cytomegalovirus (CMV) promoter was introduced into the respective EAV and PRRSV full-length cDNA clones pEAV030 and pAPRRSasc, into which an AscI restriction enzyme recognition site was inserted immediately upstream of the ORF2a start codon as described previously (23, 47, 61). To construct the chimeric full-length cDNA clone pAPRRS-EAV2ab34, cDNA fragment EAV2ab34 (representing EAV ORF2a to ORF4) was amplified from pEAV030 using the primer pair FE234asc–RE4-A5, and fragment APRRS56 (vAPRRS ORF5 to ORF6) was amplified from pAPRRS using the primer pair FE4-A5–RA14780 (Table 1). Using the purified EAV2ab34 and APRRS56 products as templates, the hybrid fragment EAV2ab34–APRRS56 was amplified via splicing overlap extension (SOE) PCR with the primer pair FE234asc–RA14780 (56). This fragment was subsequently cloned into the pCR-Blunt II-TOPO vector (Invitrogen) according to the manufacturer's recommendations in order to construct an intermediate plasmid. After digestion with the restriction enzymes AscI and XbaI (New England BioLabs, MA), the hybrid fragment EAV2ab34–APRRS56 was transferred to pAPRRSasc to yield the chimeric full-length cDNA clone pAPRRS-EAV2ab34. All constructs were verified by restriction enzyme mapping and nucleotide sequencing. The construction strategy is outlined in Fig. 1. Oligonucleotide primer sequences are listed in Table 1.

DNA transfection and rescue of virus. All experiments with live chimeric viruses and their parents were performed in a biosafety level 2 biocontainment laboratory. Full-length plasmid DNAs were isolated using the QIAprep Spin Miniprep kit (Qiagen, Hilden, Germany), verified by agarose gel (1%) electrophoresis, and quantified using a photospec-

TABLE 1 Primers used in this study

Primer[a]	Sequence (5′–3′)[b]	Application
FA12asc	GAGGCGCGCCAATGAAATGGGGTCCATGC	Generation of pAPRRSasc
RA12asc	TTGGCGCGCCTCAATTCAGGCCTAAAGTTG	
FE234asc	TGAGGCGCGCCATGGGCTTAGTGTGGTCACTG	Generation of pAPRRS-EAV234
RE4-A5	TCCCCAACATACTTAAACATTCATAGATAACATCGTTGAG	
FE4-A5	CTCAACGATGTTATCTATGAATGTTTAAGTATGTTGGGGA	
RA14780	GCATCTAGAGGTGATGAACCTCCAAGTTTCTATGG	
FA12066	CAATGATGCGTTTCGTGCGCGCC	Identification of the chimeric genome by RT-PCR
RE10766	AAGTGCACCAACAACAAGGCAAACCAAC	
RAT	GAGTGACGAGGACTCGAGCGCATGCTTTTTTTTTTTTTTT	
FA14413	CTGATCGACCTCAAAAGAGTTGTGCTTG	Detection of PRRSV ORF7 by RT-PCR
RA15497	CAATTAAATCTTACCCCCACACGGTCG	
FA6	GTATAGGTGTTGGCTCTATGCCTTG	RT-PCR amplification for sg mRNAs 2 to 5 of the APRRS sequence
RA12661	TTTACAGGTCTCGGCTTC	
RA13077	CCCTAGCTCGTCGTGATCGT	
RA13804	CGCACATGATCGACCAC	
RA14234	GCGTAGATGCTACTCAGGACATACC	
FE11	TGTATGGTGCCATATACGGCTCACCACC	RT-PCR amplification for sg mRNAs 2 to 5 of the EAV sequence
RE10474	GGAAGTGCGACGGGAAGGTGACATTAGCC	
RE10766	AAGTGCACCAACAACAAGGCAAACCAAC	
RE11153	GATAACATCGTTGAGCCCAACGTACCAGTCG	
RE11883	CCTCACAAGGTTGACTTTGCTGCCGTAG	

[a] Primer names are organized in groups. Prefixes: F, forward PCR primer; R, reverse PCR primer; A, sequence from pAPRRS (GenBank accession no. GQ330474); E, sequence from pEAV030 (GenBank accession no. NC002532).
[b] Restriction sites introduced by PCR are underlined.

trometer. Fresh MARC-145 cells in a six-well plate at approximately 60 to 80% confluence were transfected with 2 μg of plasmid per well using FuGene HD transfection reagent (Roche, Germany), followed by incubation at 37°C under 5% CO_2. The transfected cells were monitored daily. When about 80% of transfected cells displayed cytopathic effect (CPE), cell culture supernatants were harvested and were designated passage zero (P0) virus.

Indirect immunofluorescence analysis (IFA). At 48 h after inoculation at a low multiplicity of infection (MOI) of 0.01 or after transfection with full-length cDNA clones, infected or transfected cells were washed twice with phosphate-buffered saline (PBS) and were fixed in cold methanol for 15 min. After washing with PBS, the fixed cells were blocked in 1% bovine serum albumin (BSA; Sigma) at room temperature for 30 min. The cell monolayers were washed with PBS and were incubated with specific primary antibodies at 37°C for 2 h. After extensive washing with PBS, the cells were incubated with Alexa 568-labeled anti-mouse or Alexa-555-labeled anti-rabbit secondary antibodies for 1 h at room temperature. Finally, fluorescent signals were visualized using an Olympus inverted fluorescence microscope fitted with a charge-coupled device (CCD) camera.

Viral plaque assay and growth kinetics. MARC-145 or BHK-21 cells in six-well plates were inoculated with 10-fold serial dilutions of passage 3 (P3) virus. After adsorption for 1 h, the inoculum was replaced with an overlay of 1% low-melting-point agarose (Cambrex, ME) in EMEM containing 2% FBS. When the agarose overlay had solidified, the plate was inverted and placed (bottom up) in an incubator at 37°C for 3 (BHK-21) or 4 (MARC-145) days. The resulting plaques were fixed in 4% (vol/vol) formaldehyde in distilled water for 1 h and were then stained with crystal violet (5% [wt/vol] in 20% ethanol).

To examine the growth properties of chimeric viruses in MARC-145 and BHK-21 cells, a multiple-step growth curve analysis was conducted as described previously (61). Briefly, MARC-145 or BHK-21 cells were infected with P3 chimeric and parental viruses at an MOI of 0.01. At the time points indicated in Fig. 6 (12, 24, 36, 48, 60, 72, 84, and 96 h postinoculation [p.i.]), 200 μl of each culture supernatant was collected, and the supernatant was replenished with the same volume of fresh medium. Virus titrations were performed in 96-well plates with fresh cells that were incubated with 10-fold serial virus dilutions (4 replicates per dilution; 100 μl/well) for 1 h, after which the cells were washed with PBS twice and were then incubated in EMEM or MEM (for BHK-21 cells) with 2% FBS in a humidified CO_2 incubator. CPE was read at 7 or 5 (for BHK-21 cells) days p.i. Viral titers were calculated using the Reed-Muench method and were expressed as the 50% tissue culture infectious dose ($TCID_{50}$) per milliliter. Three independent experiments were carried for each virus.

RT-PCR and nucleotide sequencing. Viral genomic RNA was isolated from the supernatant of the cultured cells, which had been infected with viruses using a QIAprep viral RNA minikit (Qiagen), as instructed by the manufacturer. The complete viral genomes were amplified by reverse transcription-PCR (RT-PCR) in eight segments (primer sequences are available upon request) using avian myeloblastosis virus reverse transcriptase (TaKaRa) and *pfuUltra* II Fusion HS DNA polymerase (Stratagene), and the RT-PCR products were purified, followed by nucleotide sequence determination as described previously (25).

Total intracellular RNA was isolated by using TRIzol reagent (Invitrogen), according to the manufacturer's instructions. The sg mRNAs of chimeric and parental viruses were amplified by RT-PCR with specific primer pairs (Table 1), as described previously (7, 47). The forward primers FA6 and FEAV11 were designed to bind upstream of the 5′ UTRs of vAPRRS and vEAV030, respectively, and the reverse primers were in the 3′-terminal parts of the individual ORFs 2 to 5, such that the specific leader-body junction motif of every sg mRNA could be amplified. The RT-PCR products were cloned into the pGEM-T vector (Promega, Madison, WI) and were subjected to nucleotide sequencing.

Hybridization analysis of intracellular RNA. For a first-cycle analysis of intracellular RNA synthesis, full-length cDNA clones with a T7 RNA polymerase promoter were used. Full-length capped RNA was transcribed and introduced into BHK-21 cells by electroporation, essentially as described previously (31). Intracellular RNA was isolated at 18 h posttransfection by using a lysis buffer containing 5% lithium dodecyl sulfate, acid-phenol extraction, and isopropanol precipitation, essentially as described by van Marle and coworkers (54). Denaturing formaldehyde agarose gel electrophoresis (1.5% gel) and hybridization of dried agarose gels were performed as described previously (7). PRRSV-specific mRNAs were detected with a ^{32}P-labeled oligonucleotide probe complementary to nucle-

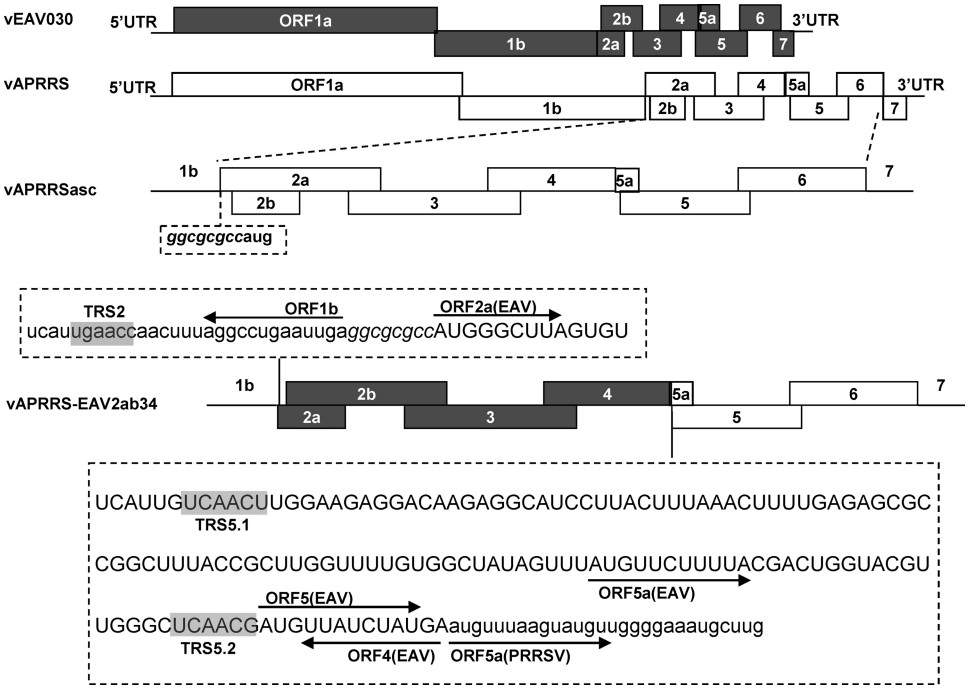

FIG 1 Schematic organization of parental and chimeric PRRSV and EAV genomes. The genomic organizations of the parental viruses, vEAV030 and vAPRRS, are represented using filled and open rectangles, respectively. The intermediate construct vAPRRSasc was generated by inserting an AscI restriction enzyme recognition sequence (*ggcgcgcc*) between the ORF1b stop codon and the ORF2a start codon. Next, the minor envelope protein-coding region of vAPRRSasc, ORF2a to ORF4, was replaced with the corresponding gene set of vEAV030, and the resultant chimeric virus was designated vAPRRS-EAV2ab34. The nucleotide sequences flanking the swapped ORFs of the chimera are shown within dashed boxes (with vAPRRS sequences in lowercase and vEAV030 sequences in uppercase).

otides (nt) 15468 to 15488 in the 3′ UTR of the viral genome sequence. Gels were exposed to phosphorimager screens, which were subsequently scanned using a Typhoon variable-mode imager (GE Healthcare). Image analysis was performed with ImageQuant TL software (GE Healthcare).

RESULTS

Generation of a viable chimeric arterivirus. Based on biochemical experiments, different PRRSV attachment proteins and corresponding cellular receptors have been proposed (4, 50). Here we addressed this issue by a genetic approach based on the exchange of the genes encoding four minor envelope proteins (E, GP2a, GP2b, GP3, GP4) of two distantly related arteriviruses displaying very different tropisms in cell culture. Because PRRSV infects only MARC-145 cells and EAV has a much broader *in vitro* tropism, a full-length chimeric cDNA clone, pAPRRS-EAV2ab34, in which the minor envelope protein genes of PRRSV (ORFs 2a to 4) were replaced by the corresponding EAV gene set was constructed (Fig. 1). Upon transfection of full-length cDNA clones into MARC-145 cells, CPE was observed on days 4 to 6 posttransfection in cells transfected with pAPRRS, pEAV030, or pAPRRS-EAVE2ab34, but not in mock-transfected control cells (data not shown). This suggested the production of viable progeny viruses from all three constructs. The supernatants harvested from these cells (P0 virus) were used for inoculation of fresh MARC-145 cells, and again vAPRRS-EAV2ab34, as well as both its parental viruses, induced CPE within 2 to 3 days.

The transfected cell monolayers were also fixed at 48 h p.i. for IFA with MAbs specific for PRRSV and EAV nonstructural and structural proteins. As shown in Fig. 2 (left), pAPRRS-EAV2ab34- and pAPRRS-transfected cells stained positive for both PRRSV nsp2 and N proteins, while pEAV030-transfected cells were negative, indicating that the CPE induced by pAPRRS-EAV2ab34 transfection was indeed PRRSV specific. As expected, EAV nsp2-specific staining was observed only in pEAV030-transfected cells, but EAV GP2b-specific staining was observed in both pEAV030- and pAPRRS-EAV2ab34-transfected cells (Fig. 2, right), ruling out the possibility that the pAPRRS-EAV2ab34 wells had been contaminated with either of the parental viruses. In conclusion, the protein expression patterns were in agreement with the chimeric nature and composition of the vAPRRS-EAV2ab34 genome.

To further confirm that the rescued viruses originated from the transfected cDNA clones, genomic RNA was extracted from P1 virus and was used for RT-PCR amplification with a pair of primers that would confirm its chimeric nature: FA12066 (located in ORF1b of vAPRRS) and RE10766 (targeting vEAV030 ORF3). Only when using the vAPRRS-EAV2ab34 genome could we amplify an RT-PCR product of the correct size (Fig. 3A). Subsequently, complete genome sequencing confirmed that the vAPRRS-EAV2ab34 genome indeed contained EAV ORFs 2a to 4 in the vAPRRS backbone, as originally engineered at the level of the full-length cDNA clone. The sequences of both PRRSV-EAV junctions (upstream of ORF2a and downstream of ORF4) were found to be identical to the originally engineered cDNA sequences (Fig. 3B).

Chimeric vAPRRS-EAV2ab34 displays an extended tropism in cell culture. To further assess the impact of the quadruple mi-

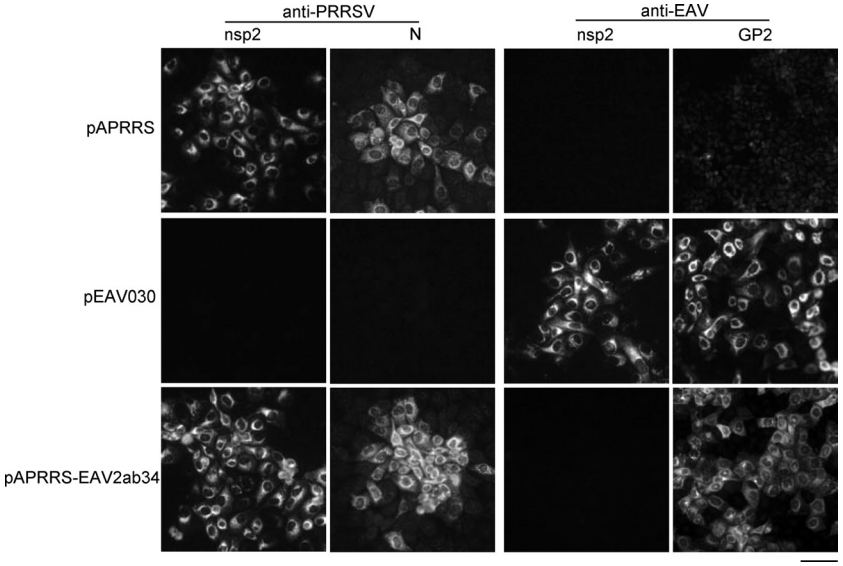

FIG 2 Expression of virus-specific markers in transfected MARC-145 cells. MARC-145 monolayers were transfected with plasmid DNAs carrying full-length EAV or PRRSV cDNAs under the control of a CMV promoter. At 48 h posttransfection, the cells were fixed and immunolabeled for PRRSV nsp2 and N, or for EAV nsp2 and GP2b, to investigate the expression of PRRSV- and EAV-specific nonstructural and structural proteins. The chimeric nature of vAPRRS-EAV2ab34 was confirmed by the fact that it expressed PRRSV nsp2 and N, as well as EAV GP2b. Bar, 100 μm.

nor envelope protein substitution, we studied the *in vitro* tropism of vAPRRS-EAV2ab34. It is well established that EAV can infect the MARC-145, BHK-21, and Vero cell lines and many others, while PRRSV can infect only MARC-145 cells. First, we inoculated fresh BHK-21 cells with vAPRRS-EAV2ab34, along with vAPRRS and vEAV030 as controls. CPE was observed for both vAPRRS-EAV2ab34 and vEAV030, but not for vAPRRS. As shown in Fig. 4A, BHK-21 cells began to round up and ultimately detached from the culture dish at 2 days p.i. IFA (Fig. 4B) confirmed that vAPPRS had failed to infect BHK-21 cells, whereas the same cells were clearly permissive for vEAV030, resulting in pronounced CPE but a lack of PRRSV-specific staining. However, when infection was performed with the chimeric virus vAPRRS-EAV2ab34, both the MARC-145 and BHK-21 cell lines were strongly labeled for PRRSV nsp2 as well as N protein. This confirmed that this chimera can efficiently infect BHK-21 cells, a property specific for the virus whose minor envelope protein genes had been transferred to the PRRSV backbone. Essentially similar results were obtained on Vero cells, a second cell line that is normally permissive to EAV but not to PRRSV (Fig. 4C).

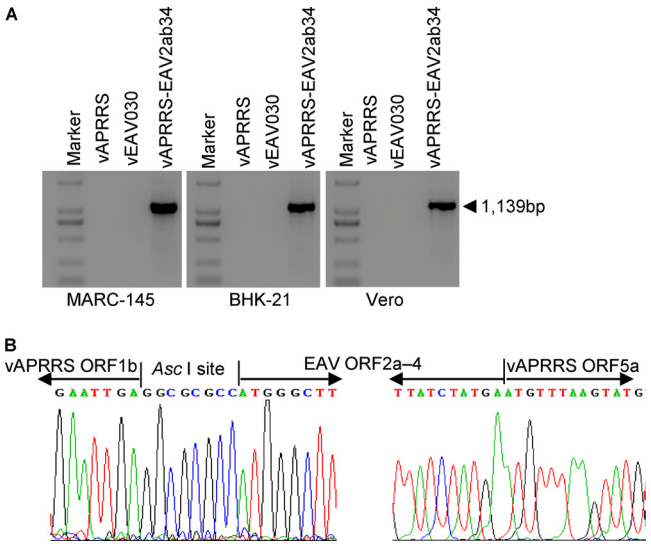

FIG 3 RT-PCR and nucleotide sequencing of the chimeric vAPRRS-EAV2ab34 genome. The P0 viruses harvested from transfected MARC-145 cells were used to inoculate fresh MARC-145, BHK-21, or Vero cells. At 48 h p.i., viral RNA was isolated from the culture supernatants and was used for RT-PCR amplification. (A) Confirmation of the chimeric nature of the vAPRRS-EAV2ab34 genome. RT-PCR was performed with the chimeric primer pair FA12066 (located in vAPRRS ORF1b)–RE10766 (in vEAV030 ORF3) to amplify a 1,139-bp product that is specific for the vAPRRS-EAV2ab34 chimera. The parental viruses were included as negative controls. (B) Sequence analysis of the junction sites in the vAPRRS-EAV2ab34 genome between PRRSV ORF1b and EAV ORF2a and between EAV ORF4 and PRRSV ORF5a. The nucleotide sequences and sequencing traces derived from these upstream and downstream fusion points are shown; the AscI restriction site and inserted EAV sequences are indicated.

To further confirm the chimeric nature of vAPRRS-EAV2ab34 progeny from BHK-21 and Vero cells, RT-PCR was performed using primer pair FA12066–RE10766. Only the vAPRRS-EAV2ab34 sample produced the anticipated amplicon (Fig. 3A). These results demonstrated that the rescued vAPRRS-EAV2ab34 chimera has an extended tropism in cell culture and that this tropism matches that of the minor envelope protein donor, EAV. Therefore, these proteins are concluded to play a key role in arterivirus attachment and entry *in vitro*, and we speculate that the same is likely also true *in vivo*.

Chimeric vAPRRS-EAV2ab34 has lost the ability to infect porcine alveolar macrophages. PRRSV and EAV can only infect cells from the monocyte/macrophage lineages of their respective natural hosts. We therefore tested whether the vAPRRS-EAV2ab34 chimera was able to infect PAM. These primary cells were inoculated with dilutions of chimeric and parental viruses, and IFA was conducted about 48 h later. The IFA results (Fig. 5A) showed that only cells infected with wild-type vAPRRS were labeled for PRRSV nsp2 and N, while cells inoculated with the chi-

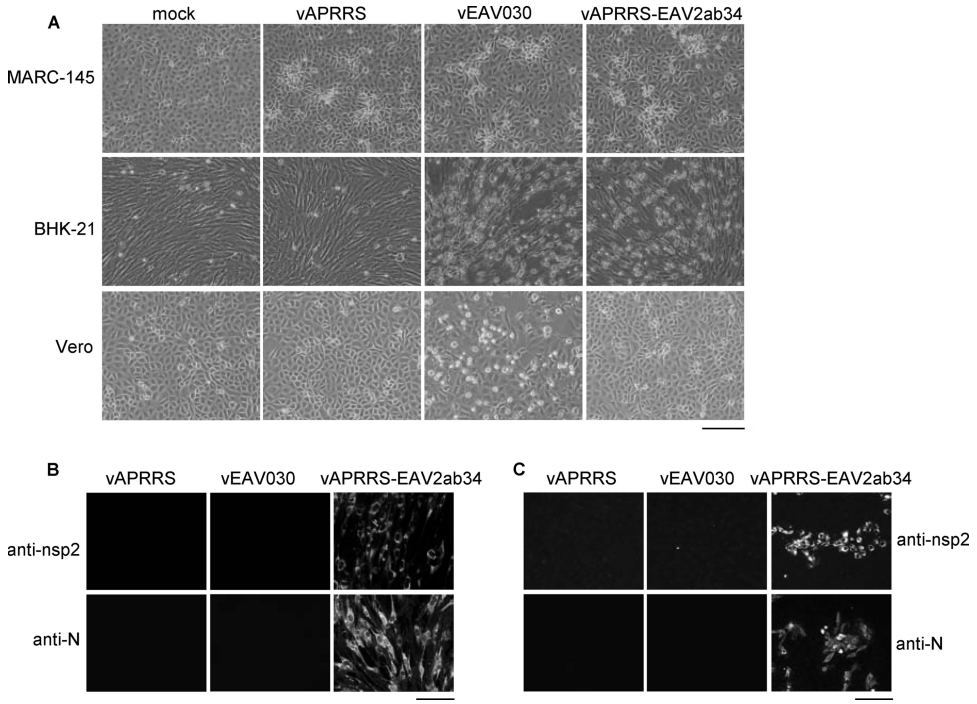

FIG 4 Productive infection of MARC-145, BHK-21, and Vero cell lines with the vAPRRS-EAV2ab34 chimera. P0 viruses harvested from transfected MARC-145 cells (the chimera and parental viruses) were used to inoculate fresh cells at an MOI of 0.01. (A) At 2 to 3 days p.i., CPE was observed in MARC-145 and BHK-21 cells but not in Vero cells. Bar, 400 μm. (B and C) Immunolabeling of BHK-21 (B) or Vero (C) cells infected with P0 virus, fixed at 48 h p.i., and stained for PRRSV nsp2 and N. Bars, 100 μm.

meric virus vAPRRS-EAV2ab34 or the parental virus vEAV030 remained negative. This indicated that vAPRRS-EAV2ab34 particles cannot productively infect PAM, which was also confirmed by RT-PCR (Fig. 5B) showing the absence of the viral genome from cells inoculated with APRRS-EAV2ab34. The observations described above demonstrated that, due to the substitution of its minor envelope proteins, the vAPRRS-EAV2ab34 chimera had lost its ability to infect PAM, which are readily infected by wild-type PRRSV particles.

Characterization of chimeric vAPRRS-EAV2ab34 propagation in MARC-145 and BHK-21cells. We next investigated the virological characteristics of the vAPRRS-EAV2ab34 chimera, using P3 viruses harvested from MARC-145 cells. Cells were infected with the chimeric and parental viruses at an MOI of 0.01. The viral titers in supernatants collected at regular intervals (12 to 96 h p.i.) were determined, and viral growth kinetics were evaluated. As shown in Fig. 6A, the chimera appeared to display somewhat accelerated growth in MARC-145 cells compared with that of the parental virus vAPRRS. Specifically, vAPRRS-EAV2ab34 reached its peak titer (2.5×10^7 $TCID_{50}$/ml) around 72 h p.i., and this titer was similar to that of vAPRRS (1.6×10^7 $TCID_{50}$/ml). This indicated that the chimeric virus replicated well in MARC-145 cells. In BHK-21 cells, which are nonpermissive for vAPRRS, the vAPRRS-EAV2ab34 chimera produced an even higher virus titer, with a peak of 2.5×10^8 $TCID_{50}$/ml, 10 times higher than that in MARC-145 cells. These results suggested that vAPRRS-EAV2ab34 replicated better in BHK-21 than in MARC-145 cells, although—not unexpectedly—vEAV030 reached the highest peak titer in both MARC-145 and BHK-21 cultures (Fig. 6A).

The plaque morphologies of chimeric and parental viruses

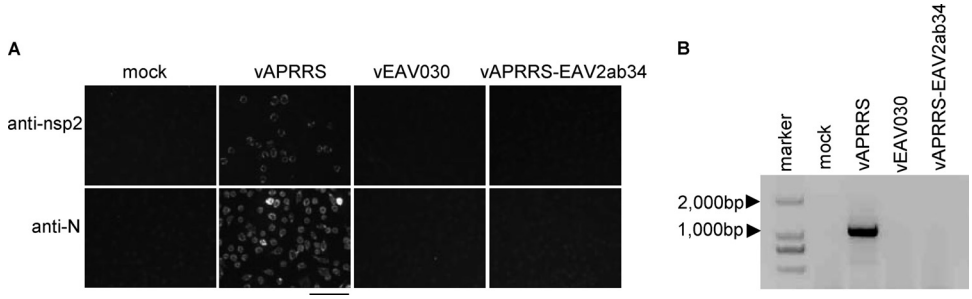

FIG 5 The vAPRRS-EAV2ab34 chimera is unable to infect PAM. (A) Fresh PAM were incubated with 100-fold-diluted chimeric and parental viruses. After about 48 h, the cell monolayers were immunolabeled for PRRSV marker proteins. Bar, 100 μm. (B) Total intracellular RNA was extracted from infected cells, and the PRRSV genomic sequence was amplified by RT-PCR with primer pair FA14413/RA15497, designed to amplify vAPRRS nucleotides 14413 to 15497.

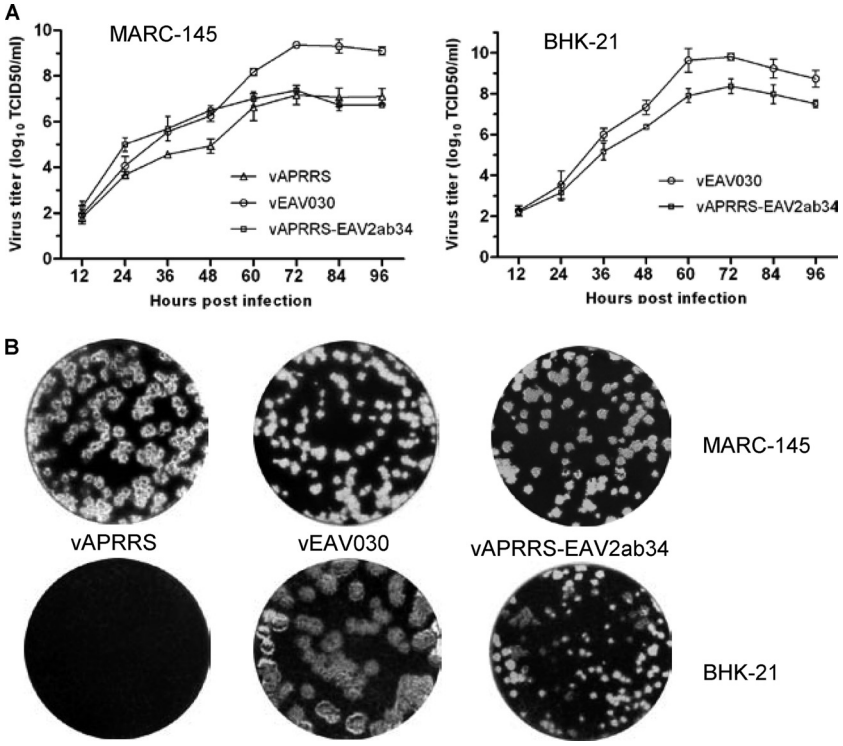

FIG 6 Virological characteristics of the vAPRRS-EAV2ab34 chimera. (A) Growth kinetics in MARC-145 and BHK-21 cells, infected at an MOI of 0.01 with P3 chimeric and parental viruses (derived from passaging in MARC-145 cells). The viral titers of each sample were determined as described in Materials and Methods. (B) Plaque morphology on MARC-145 and BHK-21 cells infected with chimeric or parental viruses as described above and overlaid with EMEM containing 2% FBS and 1% low-melting-point agarose. At 3 (for BHK-21) or 4 (for MARC-145) days p.i., plaques were visualized by crystal violet staining.

were assessed using MARC-145 cells fixed at 4 days p.i. The vAPRRS-EAV2ab34 plaques appeared similar to those of the vEAV030 donor virus, while a little smaller than those of the parental virus vAPRRS (Fig. 6B). No plaques were obtained when BHK-21 cells were infected with vAPRRS, whereas vAPRRS-EAV2ab34 produced plaques at 3 days p.i., 24 h earlier than in MARC-145 cells. However, the vAPRRS-EAV2ab34 plaques in BHK-21 cells were substantially smaller than those of vEAV030, in line with the higher titer produced by vEAV030 (Fig. 6A), but in contrast with the observation in MARC-145 cells, in which quite similar plaque sizes were seen for vEAV030 and vAPRRS-EAV2ab34.

Taken together, our results demonstrated that the replacement of the four PRRSV minor envelope proteins with their EAV counterparts resulted in a viable chimera with comparable growth kinetics in MARC-145 cells, and clearly increased virus yields in BHK-21 cells, which normally are resistant to PRRSV infection.

The transcriptional profile of the chimeric virus. Discontinuous minus-strand RNA synthesis is presumed to produce a nested set of subgenome-length templates for arterivirus sg mRNA synthesis (37, 39, 46). Base pairing between the complement of a TRS-B sequence in the nascent minus strand and the TRS-L is believed to play a critical role in determining the efficiency and precise site of leader-to-body joining (37). However, the EAV and PRRSV consensus TRS motifs are different (UCAACU and UUAACC, respectively), and in the vAPRRS-EAV2ab34 chimera, EAV-derived antisense TRS-B sequences would have to base pair with the PRRSV TRS-L sequence to produce the templates for the synthesis of sg mRNAs 3, 4, and 5 (Fig. 1). Clearly, these RNA interactions are critical for virus viability, given the fact that each of the encoded proteins is known to be crucial for the production of arterivirus progeny (29). On the other hand, it is not very clear at which level each of the sg mRNAs needs to be produced in order to obtain viable arterivirus progeny. Interestingly, the presence and use of alternative TRS-B sequences directing the synthesis of alternative versions of the same sg mRNA species have been documented, particularly for EAV mRNAs 3, 4, and 5, which are important here in the context of the vAPRRS-EAV2ab34 chimera (36).

The complement of the UCAACU consensus TRS-B motif of EAV would normally base pair with the identical EAV TRS-L sequence (38). In the vAPRRS-EAV2ab34 chimera, the TRS-L motif is the PRRSV-derived UUAACC sequence, which, in terms of TRS base pairing, essentially comes down to the loss of a base pair at position 6 and the replacement of the G-C at position 2 with G-U. Using an oligonucleotide probe complementary to the 3′ UTR of PRRSV, we investigated the synthesis of sg mRNAs by the vAPRRS-EAV2ab34 chimera in a gel hybridization analysis. As shown in Fig. 7A, the vAPRRSasc mutant virus, into which we inserted an AscI site downstream of ORF1b to create an insertion point for EAV ORFs 2a to 4 (Fig. 1), produced an sg mRNA pattern identical to that of the parental virus vAPRRS. As expected (Fig. 7A), the pattern of the chimera vAPRRS-EAV2ab34 was unchanged for the two sg mRNAs encoded downstream of this insertion site, mRNAs 6 and 7. Also, the synthesis of mRNA2, controlled by an autologous PRRSV TRS-B located in the 3′ end of ORF1b, was efficient, and as expected on the basis of the smaller size of the ORF2a-to-ORF4 gene set in EAV than in PRRSV, the

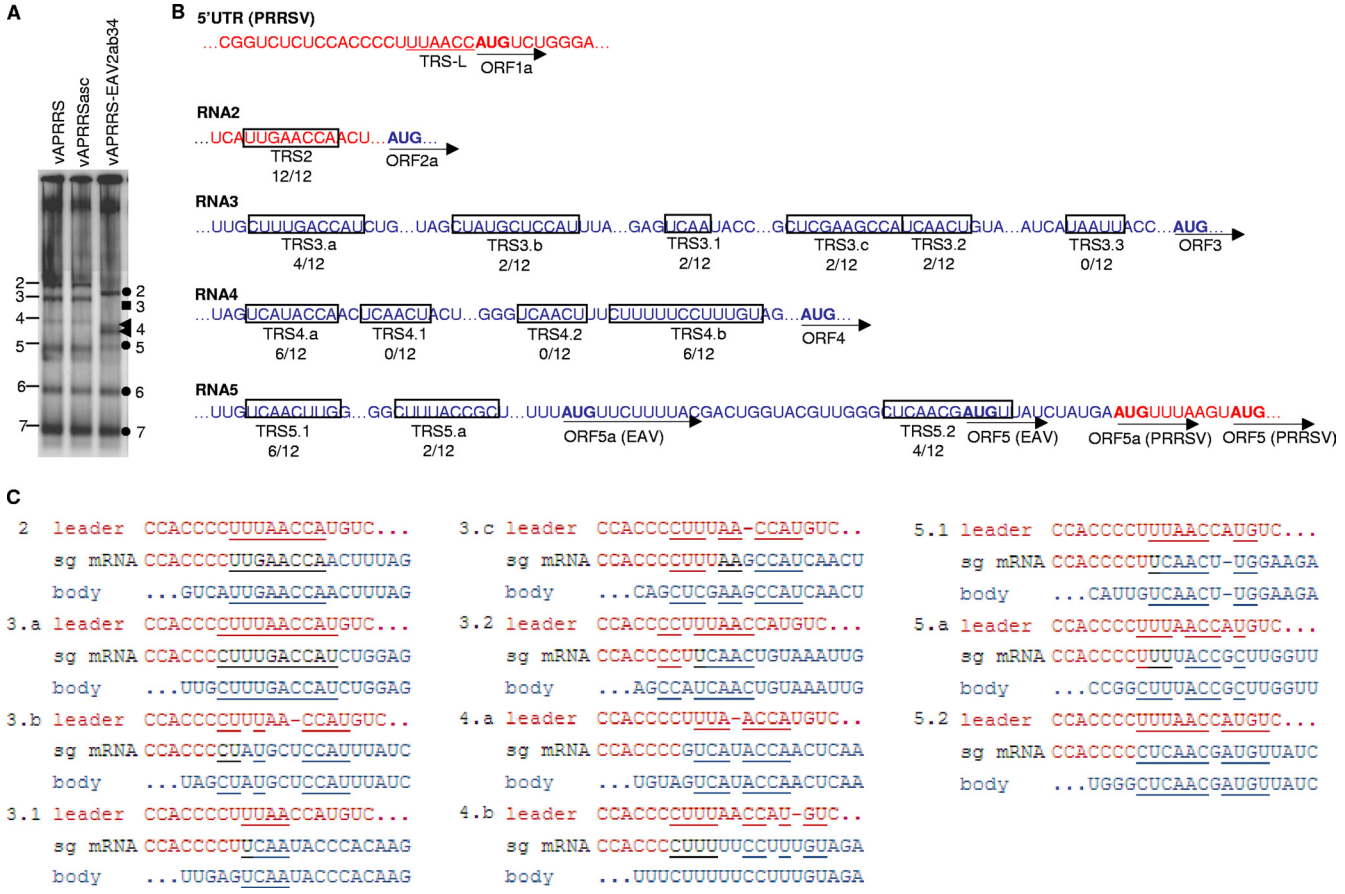

FIG 7 Analysis of vAPRRS-EAV2ab34 mRNA synthesis and leader-body junction sites. (A) Hybridization analysis of intracellular RNA isolated from BHK-21 cells transfected with full-length RNA derived from chimeric and parental cDNA constructs. The numbers on the left indicate sg mRNAs 2 to 7 of the parental virus. The circles and numbers on the right indicate the positions of sg mRNAs 2 and 5 to 7; the square indicates the diffuse sg mRNA3 band; and arrowheads point to the double band of sg mRNA4. (B) Overview of TRS-B usage of vAPRRS-EAV2ab34 as determined by RT-PCR amplification, cloning, and sequence analysis of leader-body junction sites (12 clones per mRNA). The TRS-L region of the PRRSV 5′ UTR is shown at the top, and the TRS-L core sequence is underlined. The junction sites identified for each of mRNAs 2 to 5 are summarized; boxed regions indicate the possibilities of base pairing with the TRS-L sequence. Previously identified EAV TRS-B motifs (36) are designated 3.1, 3.2, etc., whereas newly discovered TRS-B-like sequences are named 3.a, 3.b, etc. The frequency with which each junction was encountered in the 12 cDNA clones analyzed is given below the TRS-B name. The initiation codons of the various ORFs are in boldface. PRRSV-derived sequences are shown in red, while EAV-derived sequences are shown in blue. (C) Analysis of vAPRRS-EAV2ab34 TRSs and leader-body junction sites and their flanking sequences. The sequences in the TRS-L and TRS-B regions are shown in red and blue, respectively, whereas the composition of the mRNA sequence found is shown in between (black nucleotides can be derived from either TRS-B or TRS-L). The underlined nucleotides represent base-pairing possibilities (including potential G-U base pairs; a single insertion was tolerated when necessary).

resulting mRNA2 was about 300 nucleotides shorter than the corresponding transcript of the parental virus.

The interpretation of our findings for the three mRNAs controlled by EAV-derived TRS-B motifs was less straightforward. sg mRNA3, predicted to be about 130 nucleotides smaller than its equivalent from its vAPRRSasc parent, appeared as a diffuse smear, potentially consisting of multiple RNA species. A double band was observed at the predicted position of mRNA4 (~2,350 nt), and in particular, the smaller of these two mRNAs appeared to be efficiently produced. RNA5 was observed as a band of an intensity about equal to that of the parental virus, but slightly larger, as predicted from the sequence of the chimeric virus, assuming that EAV TRS5.1 (36) would be used to produce this transcript.

Although we consider an extensive analysis of the synthesis of mRNAs by the chimeric virus to be beyond the scope of this study, we characterized the sg mRNAs expressing the EAV-derived structural protein genes in some more detail. To this end, the leader-body junction sites of sg mRNAs 2, 3, 4, and 5 of the chimeric virus were amplified by RT-PCR and cloned for nucleotide sequence analysis (Fig. 7B and C). This showed that, as expected from its position inside PRRSV ORF1b (Fig. 1), the TRS-B used to produce mRNA2 had not changed in the chimeric virus. For mRNA3 of the chimeric virus (Fig. 7B and C), the use of the two previously documented dominant TRS-B sequences (TRS3.1 and TRS3.2) was observed (7, 36), but various alternative junction sites (designated TRS3.a, -3.b, and -3.c) also appeared to be used. In our opinion, the mixture of sg mRNA3 species identified, and their individual low abundances, adequately explains the lack of a prominent RNA3 band in Fig. 7A. The results for mRNA4 remained somewhat puzzling, since two novel TRS-B-like motifs (TRS4.a and -4.b) with only a moderate match with the PRRSV TRS-L were found to be used, whereas the original EAV TRS-B4.1 and TRS-B4.2 appeared to remain silent. In the case of mRNA5, the dominant EAV TRS-B (TRS5.1) (36) was found in 6 out of 12

clones, but TRS5.2 and a novel junction site located between TRS5.1 and TRS5.2 were also used (TRS5.a [Fig. 7B]). Furthermore, the translation of the various mRNA5 species raised a number of questions, both mechanistically and in terms of the encoded polypeptides, which are discussed below.

In general, the conclusion that the requirements for TRS base pairing and translation of ORFs 3, 4, and 5 or 5a in vAPRRS-EAV2ab34 must be relatively relaxed seems justified. While tolerating mismatches in TRS base pairing, the PRRSV leader sequence could be attached to both known EAV TRS-B motifs and to novel sequences. The latter resembled the UUAACC TRS-L motif of PRRSV to various extents, but none of them was a perfect match (Fig. 7C). Still, the population of at least 10 different sg mRNAs produced to express ORFs 3 to 5 apparently sufficed to ensure the viability of the vAPRRS-EAV2ab34 chimera documented in this study.

Genetic stability of the vAPRRS-EAV2ab34 chimeric virus. There is very limited overall sequence similarity between EAV and PRRSV, and the structural-protein-coding ORFs differ in length. Additionally, the interactions between the various envelope proteins, and between the N protein and RNA, are essential for EAV and PRRSV assembly and infectivity. Consequently, we anticipated that the chimeric virus might evolve during passaging and could acquire adaptive mutations that would further improve its replicative potential. We therefore assessed the stability of the vAPRRS-EAV2ab34 chimera by performing eight consecutive passages in fresh MARC-145 cells, each time inoculating with a 1,000-fold dilution of the supernatant of the previous passage. Ultimately, the P8 viral RNA was extracted, amplified in its entirety by RT-PCR, and subjected to nucleotide sequencing, which revealed three nonsynonymous replicase point mutations (Glu-2512 → Asp in nsp9, Arg-3881 → Pro and Lys-3902 → Thr in nsp12) and one synonymous point mutation (U → C) at nucleotide 198 in the inserted EAV ORF3. In particular, nucleotide sequencing demonstrated that the heterologous ORF2a-to-ORF4 region had remained genetically stable for eight passages, and no nonsynonymous mutations were detected in any of the structural-protein-coding sequences (data not shown).

DISCUSSION

Arteriviruses can cause various clinical symptoms ranging from lethal to asymptomatic persistent infection in susceptible host animals (42). Of the four family members, EAV and PRRSV stand out for economic reasons, and the latter virus has rapidly become one of the most economically important swine pathogens worldwide. Furthermore, EAV and PRRSV have attracted attention due to a variety of molecular biological features and have been developed into important models for basic research on arteriviruses and nidoviruses at large. Entry is the first step of the viral replicative cycle, and dissection of this process will be of great significance for controlling arterivirus infection. However, the molecular interactions involved in arterivirus attachment and entry have remained poorly understood and "controversial," to say the least. It is generally accepted that PRRSV enters host cells via receptor-mediated endocytosis (22, 49). Several cellular molecules have been proposed as potential cellular receptors, including heparan sulfate, pSn, CD151, CD163, and vimentin (1, 13, 21, 40, 51). Of these cellular molecules, pSn has been most extensively studied, but its role was challenged by the discovery of another potential receptor, CD163, a macrophage-specific protein in the scavenger receptor cysteine-rich (SRCS) superfamily (1). Van Breedam et al. proposed that pSn is the authentic receptor for virus internalization, while CD163 may function as a downstream mediator of entry, e.g., during genome uncoating (49, 53). While both putative receptors could be utilized for PRRSV entry, e.g., acting as the receptor and coreceptor, as described for human immunodeficiency virus (8), it remains difficult to reconcile this model with the absence of pSn in MARC-145 cells, the sole cell line supporting PRRSV propagation *in vitro* (13). Compared to the studies on (putative) cellular receptors, there are only a few publications about the arterivirus attachment protein(s). PRRSV GP5 was long believed to be the attachment protein, against which most of the neutralizing antibodies are targeted (35). However, previous studies with chimeric arteriviruses suggested that the ectodomains of GP5 and/or M do not mediate attachment (11, 55). Van Breedam et al. reported that the GP5/M complex, but not the minor envelope proteins, strongly interacts with pSn in a sialic acid-dependent manner (50). However, Das and colleagues found that the minor envelope proteins GP4 and GP2a interacted specifically with *in vitro*-expressed CD163, with which GP5 interacted only weakly (4). Both groups provided solid biochemical evidence, but definitive genetic or virological support for their findings was lacking and is required in order to clarify this controversy regarding arterivirus entry.

Full-length infectious cDNA clones of arteriviruses have greatly facilitated the molecular dissection of virus replication (9, 27, 34, 52, 62). EAV and PRRSV display very different tropisms in cell culture. We hypothesized that chimeric arteriviruses carrying different combinations of envelope proteins could aid in identifying the viral attachment protein (42). By using an EAV infectious cDNA clone as a backbone, chimeras in which the GP5 ectodomain was replaced by comparable sequences of related and unrelated RNA viruses had been developed previously, and two viable chimeric viruses containing the GP5 ectodomains of PRRSV and LDV were obtained (11). However, these EAV chimeras retained the capacity to infect BHK-21 cells, suggesting that the GP5 ectodomain did not play a significant role in determining EAV tropism. Similar conclusions were drawn for the ectodomain of the M protein (55). These results implied that the minor rather than the major envelope protein(s) might mediate arterivirus attachment.

In our present study, we completely replaced PRRSV ORFs 2a to 4 with their EAV counterparts, and a viable chimeric virus was rescued. To our knowledge, this is the first successful cross-species exchange of complete arterivirus genes. More importantly, the chimeric virus displayed an extended *in vitro* tropism compared to that of its PRRSV parent, a tropism that is characteristic of EAV, the donor of its minor envelope proteins. Moreover, the chimera lost the capacity to infect the natural PRRSV target cell (PAM), demonstrating that the exchanged proteins must play a key role in arterivirus attachment and/or entry in cell culture. As a follow-up, it would be interesting to explore the exchange of individual members of the ORF2a-to-ORF4 gene set, but unfortunately, the arterivirus genome is organized in a compact manner (Fig. 1), and ORFs 2a to 4 share long overlapping sequences with their neighbors, rendering the exchange of single intact ORFs technically challenging (61).

Our results create new possibilities for the functional characterization of arterivirus minor envelope proteins, which are poorly understood compared to the major envelope proteins. It

was first demonstrated for EAV that all of the minor envelope proteins are crucial for infectivity, since a deficiency in any one of them abolished the production of infectious progeny, even though they were found to be dispensable for the assembly of a (noninfectious) core particle (59). Similar observations were subsequently made for PRRSV (60). Here we provide the first genetic and virological evidence demonstrating that one of the minor envelope proteins, or (more likely) a combination of several of these proteins, plays key roles in viral attachment and entry.

Although not the primary topic of our study, the properties of the chimeric virus also provided additional insights into arterivirus sg mRNA synthesis. TRS base-pairing possibilities, flanking sequences of TRS motifs, and local RNA structure have all been postulated to influence the use of specific TRS-B motifs (37, 39, 46). Each of these parameters can be affected by mutations like those triggered here by the construction of the chimeric virus, which may trigger or enhance the generation of sg RNAs from noncanonical TRS-B motifs, as also observed in previous studies when regular TRS-B motifs of EAV were inactivated by targeted mutagenesis or when foreign sequences were inserted into the EAV genome (10, 36, 38). For several EAV mRNAs (mRNAs 3, 4, and 5), the natural existence of multiple "subspecies" has been documented previously, although their individual contributions to the expression of the respective structural proteins have not been studied. Likewise, in this study, the importance of each of the mRNA subspecies detected (mRNAs 3, 4, and 5) is difficult to assess, if only because the analysis of 12 clones per mRNA is not sufficient to obtain a reliable measurement of their relative abundances. In-depth analysis of vAPRRS-EAV2ab34 mRNA synthesis is clearly beyond the scope of this study, which focuses on viral structural proteins and tropism, but is certainly an interesting topic for follow-up studies.

Whereas the expression of ORFs 3 and 4 from their respective alternative sg mRNAs seems straightforward, the same cannot be said about ORF5a and ORF5 (Fig. 7B). Arterivirus ORF5a was identified only recently (17, 19), and its existence was unknown at the time of vAPRRS-EAV2ab34 design. PRRSV ORF5a and ORF5 are both intact (Fig. 1 and 7B) and can in principle be translated from the sg mRNA produced from TRS5.2, although two other AUG codons (from the EAV insert) precede their initiation codons in this mRNA (including the EAV ORF5 start codon). For the transcripts derived from TRS5.1 and TRS5.a (Fig. 7B), the situation is even more complex, since these are now known to contain the 5′ part of EAV ORF5a, which became fused in frame to the downstream PRRSV ORF5 (Fig. 7B), encoding an N-terminally extended PRRSV GP5 that may not be functional, since its signal sequence is no longer positioned at the N terminus of the polypeptide. A detailed analysis of the relative abundances and translation efficiencies of the various vAPRRS-EAV2ab34 mRNA5 subspecies will be required in order to begin to understand how the chimeric virus is able to produce sufficient amounts of the ORF5a and GP5 proteins.

Despite the questions remaining on vAPRRS-EAV2ab34 sg mRNA synthesis and translation, we believe that our findings may open new avenues for PRRSV vaccine improvement, since the current modified live vaccine (MLV) can be amplified only in MARC-145 cells, which yield low virus titers. The chimeric virus described here can productively infect BHK-21 cells, and better yet, a peak titer of 2.5×10^8 $TCID_{50}$/ml, 10 times higher than that of its vAPRRS parent, was measured in the MARC-145 cell line. In addition, the chimeric nature of this recombinant virus could provide a blueprint for the rational design of vaccines that can be used to differentiate between infected and vaccinated animals, which is thought to be pivotal for the eradication of PRRSV in swine herds. We note that the *in vivo* tropism of the vAPRRS-EAV2ab34 chimera described in this paper likely differs from that of its PRRSV parent. The fact that the chimeric virus is unable to infect PAM, the natural target cell of PRRSV, suggests that it is not likely able to productively infect swine. Whether horses or other hosts are susceptible to infection with the chimeric virus is uncertain at this time and will depend on the requirements for host cell factors in addition to the receptor recognized by the EAV minor envelope proteins, which remains to be identified. Before any further use of this kind of chimeric virus in vaccine studies is considered, the susceptibility of a broader spectrum of host cells from a variety of animal hosts, including primary cells, should be investigated. Subsequently, also from a biosafety perspective, small-scale animal experiments may be required in order to fully understand the *in vivo* properties of the vAPRRS-EAV2ab34 chimera. Such studies would be permissible in biosafety level 2 biocontainment facilities.

ACKNOWLEDGMENTS

We thank Ying Fang for generously providing the monoclonal antibody against the PRRSV nsp2 and N proteins.

This work was supported by the Natural Sciences Foundation of China (30972204 and 30901078) and the EU Framework Programme 7 Project (245141).

REFERENCES

1. **Calvert JG, et al.** 2007. CD163 expression confers susceptibility to porcine reproductive and respiratory syndrome viruses. J. Virol. **81**:7371–7379.
2. **Cavanagh D.** 1997. *Nidovirales*: a new order comprising *Coronaviridae* and *Arteriviridae*. Arch. Virol. **142**:629–633.
3. **Darwich L, Diaz I, Mateu E.** 2010. Certainties, doubts and hypotheses in porcine reproductive and respiratory syndrome virus immunobiology. Virus Res. **154**:123–132.
4. **Das PB, et al.** 2010. The minor envelope glycoproteins GP2a and GP4 of porcine reproductive and respiratory syndrome virus interact with the receptor CD163. J. Virol. **84**:1731–1740.
5. **Delputte PL, Costers S, Nauwynck HJ.** 2005. Analysis of porcine reproductive and respiratory syndrome virus attachment and internalization: distinctive roles for heparan sulphate and sialoadhesin. J. Gen. Virol. **86**: 1441–1445.
6. **Delputte PL, Nauwynck HJ.** 2004. Porcine arterivirus infection of alveolar macrophages is mediated by sialic acid on the virus. J. Virol. **78**:8094–8101.
7. **den Boon JA, Kleijnen MF, Spaan WJ, Snijder EJ.** 1996. Equine arteritis virus subgenomic mRNA synthesis: analysis of leader-body junctions and replicative-form RNAs. J. Virol. **70**:4291–4298.
8. **Deng H, et al.** 1996. Identification of a major co-receptor for primary isolates of HIV-1. Nature **381**:661–666.
9. **de Vries AA, et al.** 2000. Genetic manipulation of equine arteritis virus using full-length cDNA clones: separation of overlapping genes and expression of a foreign epitope. Virology **270**:84–97.
10. **de Vries AA, Glaser AL, Raamsman MJ, Rottier PJ.** 2001. Recombinant equine arteritis virus as an expression vector. Virology **284**:259–276.
11. **Dobbe JC, van der Meer Y, Spaan WJ, Snijder EJ.** 2001. Construction of chimeric arteriviruses reveals that the ectodomain of the major glycoprotein is not the main determinant of equine arteritis virus tropism in cell culture. Virology **288**:283–294.
12. **Duan X, Nauwynck HJ, Favoreel H, Pensaert MB.** 1998. Porcine reproductive and respiratory syndrome virus infection of alveolar macrophages can be blocked by monoclonal antibodies against cell surface antigens. Adv. Exp. Med. Biol. **440**:81–88.
13. **Duan X, Nauwynck HJ, Favoreel HW, Pensaert MB.** 1998. Identification of a putative receptor for porcine reproductive and respiratory syndrome virus on porcine alveolar macrophages. J. Virol. **72**:4520–4523.

14. **Duan X, Nauwynck HJ, Pensaert MB.** 1997. Effects of origin and state of differentiation and activation of monocytes/macrophages on their susceptibility to porcine reproductive and respiratory syndrome virus (PRRSV). Arch. Virol. **142**:2483–2497.
15. **Faaberg KS, Even C, Palmer GA, Plagemann PG.** 1995. Disulfide bonds between two envelope proteins of lactate dehydrogenase-elevating virus are essential for viral infectivity. J. Virol. **69**:613–617.
16. **Fang Y, Snijder EJ.** 2010. The PRRSV replicase: exploring the multifunctionality of an intriguing set of nonstructural proteins. Virus Res. **154**:61–76.
17. **Firth AE, et al.** 2011. Discovery of a small arterivirus gene that overlaps the GP5 coding sequence and is important for virus production. J. Gen. Virol. **92**(Pt 2):1097–1106.
18. **Godeny EK, de Vries AA, Wang XC, Smith SL, de Groot RJ.** 1998. Identification of the leader-body junctions for the viral subgenomic mRNAs and organization of the simian hemorrhagic fever virus genome: evidence for gene duplication during arterivirus evolution. J. Virol. **72**: 862–867.
19. **Johnson CR, Griggs TF, Gnanandarajah JS, Murtaugh MP.** 2011. Novel structural protein in porcine reproductive and respiratory syndrome virus encoded in an alternative open reading frame 5 present in all arteriviruses. J. Gen. Virol. **92**(Pt 2):1107–1116.
20. **Kim HS, Kwang J, Yoon IJ, Joo HS, Frey ML.** 1993. Enhanced replication of porcine reproductive and respiratory syndrome (PRRS) virus in a homogeneous subpopulation of MA-104 cell line. Arch. Virol. **133**:477–483.
21. **Kim JK, Fahad AM, Shanmukhappa K, Kapil S.** 2006. Defining the cellular target(s) of porcine reproductive and respiratory syndrome virus blocking monoclonal antibody 7G10. J. Virol. **80**:689–696.
22. **Kreutz LC, Ackermann MR.** 1996. Porcine reproductive and respiratory syndrome virus enters cells through a low pH-dependent endocytic pathway. Virus Res. **42**:137–147.
23. **Lee C, Calvert JG, Welch SK, Yoo D.** 2005. A DNA-launched reverse genetics system for porcine reproductive and respiratory syndrome virus reveals that homodimerization of the nucleocapsid protein is essential for virus infectivity. Virology **331**:47–62.
24. **Li Y, et al.** 2007. Emergence of a highly pathogenic porcine reproductive and respiratory syndrome virus in the Mid-Eastern region of China. Vet. J. **174**:577–584.
25. **Lv J, Zhang J, Sun Z, Liu W, Yuan S.** 2008. An infectious cDNA clone of a highly pathogenic porcine reproductive and respiratory syndrome virus variant associated with porcine high fever syndrome. J. Gen. Virol. **89**: 2075–2079.
26. **Meng XJ, Paul PS, Morozov I, Halbur PG.** 1996. A nested set of six or seven subgenomic mRNAs is formed in cells infected with different isolates of porcine reproductive and respiratory syndrome virus. J. Gen. Virol. **77**(Pt 6):1265–1270.
27. **Meulenberg JJ, Bos-de Ruijter JN, Wensvoort G, Moormann RJ.** 1998. An infectious cDNA clone of porcine reproductive and respiratory syndrome virus. Adv. Exp. Med. Biol. **440**:199–206.
28. **Molenkamp R, Greve S, Spaan WJ, Snijder EJ.** 2000. Efficient homologous RNA recombination and requirement for an open reading frame during replication of equine arteritis virus defective interfering RNAs. J. Virol. **74**:9062–9070.
29. **Molenkamp R, et al.** 2000. The arterivirus replicase is the only viral protein required for genome replication and subgenomic mRNA transcription. J. Gen. Virol. **81**:2491–2496.
30. **Nauwynck HJ, Duan X, Favoreel HW, Van Oostveldt P, Pensaert MB.** 1999. Entry of porcine reproductive and respiratory syndrome virus into porcine alveolar macrophages via receptor-mediated endocytosis. J. Gen. Virol. **80**(Pt 2):297–305.
31. **Nedialkova DD, Gorbalenya AE, Snijder EJ.** 2010. Arterivirus Nsp1 modulates the accumulation of minus-strand templates to control the relative abundance of viral mRNAs. PLoS Pathog. **6**:e1000772.
32. **Nelsen CJ, Murtaugh MP, Faaberg KS.** 1999. Porcine reproductive and respiratory syndrome virus comparison: divergent evolution on two continents. J. Virol. **73**:270–280.
33. **Neumann EJ, et al.** 2005. Assessment of the economic impact of porcine reproductive and respiratory syndrome on swine production in the United States. J. Am. Vet. Med. Assoc. **227**:385–392.
34. **Nielsen HS, et al.** 2003. Generation of an infectious clone of VR-2332, a highly virulent North American-type isolate of porcine reproductive and respiratory syndrome virus. J. Virol. **77**:3702–3711.
35. **Ostrowski M, et al.** 2002. Identification of neutralizing and nonneutralizing epitopes in the porcine reproductive and respiratory syndrome virus GP5 ectodomain. J. Virol. **76**:4241–4250.
36. **Pasternak AO, Gultyaev AP, Spaan WJ, Snijder EJ.** 2000. Genetic manipulation of arterivirus alternative mRNA leader-body junction sites reveals tight regulation of structural protein expression. J. Virol. **74**:11642–11653.
37. **Pasternak AO, Spaan WJ, Snijder EJ.** 2006. Nidovirus transcription: how to make sense. . .? J. Gen. Virol. **87**:1403–1421.
38. **Pasternak AO, van den Born E, Spaan WJ, Snijder EJ.** 2001. Sequence requirements for RNA strand transfer during nidovirus discontinuous subgenomic RNA synthesis. EMBO J. **20**:7220–7228.
39. **Sawicki SG, Sawicki DL, Siddell SG.** 2007. A contemporary view of coronavirus transcription. J. Virol. **81**:20–29.
40. **Shanmukhappa K, Kim JK, Kapil S.** 2007. Role of CD151, a tetraspanin, in porcine reproductive and respiratory syndrome virus infection. Virol. J. **4**:62.
41. **Snijder EJ, Dobbe JC, Spaan WJ.** 2003. Heterodimerization of the two major envelope proteins is essential for arterivirus infectivity. J. Virol. **77**:97–104.
42. **Snijder EJ, Meulenberg JJ.** 1998. The molecular biology of arteriviruses. J. Gen. Virol. **79**(Pt 5):961–979.
43. **Snijder EJ, Spaan WJM.** 2007. Arteriviruses, p 1337–1355. *In* Knipe DM et al (ed), Fields virology, 5th ed. Lippincott, Williams & Wilkins, Philadelphia, PA.
44. **Snijder EJ, van Tol H, Pedersen KW, Raamsman MJ, de Vries AA.** 1999. Identification of a novel structural protein of arteriviruses. J. Virol. **73**: 6335–6345.
45. **Snijder EJ, Wassenaar AL, Spaan WJ.** 1994. Proteolytic processing of the replicase ORF1a protein of equine arteritis virus. J. Virol. **68**:5755–5764.
46. **Sola I, Mateos-Gomez PA, Almazan F, Zuniga S, Enjuanes L.** 2011. RNA-RNA and RNA-protein interactions in coronavirus replication and transcription. RNA Biol. **8**:237–248.
47. **Tian D, Zheng H, Zhang R, Zhuang J, Yuan S.** 2011. Chimeric porcine reproductive and respiratory syndrome viruses reveal full function of genotype 1 envelope proteins in the backbone of genotype 2. Virology **412**:1–8.
48. **Tian K, et al.** 2007. Emergence of fatal PRRSV variants: unparalleled outbreaks of atypical PRRS in China and molecular dissection of the unique hallmark. PLoS One **2**:e526.
49. **Van Breedam W, et al.** 2010. Porcine reproductive and respiratory syndrome virus entry into the porcine macrophage. J. Gen. Virol. **91**:1659–1667.
50. **Van Breedam W, et al.** 2010. The M/GP(5) glycoprotein complex of porcine reproductive and respiratory syndrome virus binds the sialoadhesin receptor in a sialic acid-dependent manner. PLoS Pathog. **6**:e1000730.
51. **Vanderheijden N, et al.** 2003. Involvement of sialoadhesin in entry of porcine reproductive and respiratory syndrome virus into porcine alveolar macrophages. J. Virol. **77**:8207–8215.
52. **van Dinten LC, den Boon JA, Wassenaar AL, Spaan WJ, Snijder EJ.** 1997. An infectious arterivirus cDNA clone: identification of a replicase point mutation that abolishes discontinuous mRNA transcription. Proc. Natl. Acad. Sci. U. S. A. **94**:991–996.
53. **Van Gorp H, Van Breedam W, Delputte PL, Nauwynck HJ.** 2008. Sialoadhesin and CD163 join forces during entry of the porcine reproductive and respiratory syndrome virus. J. Gen. Virol. **89**:2943–2953.
54. **van Marle G, van Dinten LC, Spaan WJ, Luytjes W, Snijder EJ.** 1999. Characterization of an equine arteritis virus replicase mutant defective in subgenomic mRNA synthesis. J. Virol. **73**:5274–5281.
55. **Verheije MH, Welting TJ, Jansen HT, Rottier PJ, Meulenberg JJ.** 2002. Chimeric arteriviruses generated by swapping of the M protein ectodomain rule out a role of this domain in viral targeting. Virology **303**:364–373.
56. **Warrens AN, Jones MD, Lechler RI.** 1997. Splicing by overlap extension by PCR using asymmetric amplification: an improved technique for the generation of hybrid proteins of immunological interest. Gene **186**:29–35.
57. **Wensvoort G, et al.** 1991. Mystery swine disease in The Netherlands: the isolation of Lelystad virus. Vet. Q. **13**:121–130.
58. **Wieringa R, de Vries AA, Rottier PJ.** 2003. Formation of disulfide-linked complexes between the three minor envelope glycoproteins (GP2b, GP3, and GP4) of equine arteritis virus. J. Virol. **77**:6216–6226.
59. **Wieringa R, et al.** 2004. Structural protein requirements in equine arteritis virus assembly. J. Virol. **78**:13019–13027.
60. **Wissink EH, et al.** 2005. Envelope protein requirements for the assembly of infectious virions of porcine reproductive and respiratory syndrome virus. J. Virol. **79**:12495–12506.

61. **Yu D, et al.** 2009. Reverse genetic manipulation of the overlapping coding regions for structural proteins of the type II porcine reproductive and respiratory syndrome virus. Virology **383**:22–31.
62. **Yuan S, Wei Z.** 2008. Construction of infectious cDNA clones of PRRSV: separation of coding regions for nonstructural and structural proteins. Sci. China C Life Sci. **51**:271–279.
63. **Zevenhoven-Dobbe JC, Greve S, van Tol H, Spaan WJ, Snijder EJ.** 2004. Rescue of disabled infectious single-cycle (DISC) equine arteritis virus by using complementing cell lines that express minor structural glycoproteins. J. Gen. Virol. **85**:3709–3714.
64. **Zhou YJ, et al.** 2008. Highly virulent porcine reproductive and respiratory syndrome virus emerged in China. Transbound. Emerg. Dis. **55**:152–164.
65. **Ziebuhr J, Snijder EJ, Gorbalenya AE.** 2000. Virus-encoded proteinases and proteolytic processing in the *Nidovirales*. J. Gen. Virol. **81**:853–879.